

# Directional wave measurements using an autonomous vessel

Lars R. Hole<sup>1</sup>  · Ilker Fer<sup>2,3</sup> · David Peddie<sup>3</sup>

Received: 29 February 2016 / Accepted: 28 June 2016 / Published online: 1 August 2016  
© The Author(s) 2016. This article is published with open access at Springerlink.com

**Abstract** An autonomous vessel, the Offshore Sensing Sailbuoy, was used for wave measurements near the Ekofisk oil platform complex in the North Sea (56.5° N, 3.2° E, operated by ConocoPhillips) from 6 to 20 November 2015. Being 100 % wind propelled, the Sailbuoy has two-way communication via the Iridium network and has the capability for missions of 6 months or more. It has previously been deployed in the Arctic, Norwegian Sea and the Gulf of Mexico, but the present study was the first test for wave measurements. During the campaign the Sailbuoy held position about 20 km north-east of Ekofisk (on the lee side) during rough conditions. Mean wind speed measured at Ekofisk during the campaign was 9.8 m/s, with a maximum of 20.4 m/s, with wind mostly from south and southwest. A Datawell MOSE G1000 GPS-based 2 Hz wave sensor was mounted on the Sailbuoy. Mean significant wave height ( $H_s$  1 min) measured was 3 m, whereas maximum  $H_s$  was 6 m. Mean wave period was 7.7 s, while maximum wave height,  $H_{max}$ , was 12.6 m. These measurements have been compared with non-directional Waverider observations at the Ekofisk

complex. The agreement between the two data sets was very good, with a mean percent absolute error of 7 % and a linear correlation coefficient of 0.97. The wave frequency spectra measured by the two instruments compared very well, except for low  $H_s$  (~1 m), where the motion of the vessel seemed to influence the measurements. Nevertheless, the Sailbuoy performed well during this campaign, and results suggest that it is a suitable platform for wave measurements in a broad range of sea conditions.

**Keywords** Surface · Waves · Directional · Autonomous · Vessel · Measurements · North Sea

## 1 Introduction

Accurate ocean wave observations and forecasts are in increasing demand, and of interest to users involved in the offshore industry, shipping, offshore wind energy industry and prospecting of bridges, roads and other near shore constructions. For example, along the coast of Norway, several fjord-crossing road construction projects involving long bridges are under way, and detailed mapping of the local wave climate is required.

The North Sea is an area with rough ocean conditions year round (Grabemann and Weisse 2008). A significant wave height,  $H_s$ , exceeding 19 m in the Northern North Sea is suggested to be realistic in the worst case scenarios described by Reistad et al. (2005). Aarnes et al. (2012) suggest a 100 year return value of  $H_s$  for the North Sea of 16–20 m, depending on method. However, there is a negative trend in  $H_s$  and wind speed in the region in recent decades (Young et al.

---

This article is part of the Topical Collection on the *14th International Workshop on Wave Hindcasting and Forecasting in Key West, Florida, USA, November 8–13, 2015*

---

Responsible Editor: Val Swail

---

✉ Lars R. Hole  
lrh@met.no

<sup>1</sup> Norwegian Meteorological Institute, Allegaten 70,  
5007 Bergen, Norway

<sup>2</sup> Geophysical Institute, University of Bergen, Bergen, Norway

<sup>3</sup> Offshore Sensing AS, Bergen, Norway

**Fig. 1** Sketch of the Sailbuoy with major components highlighted

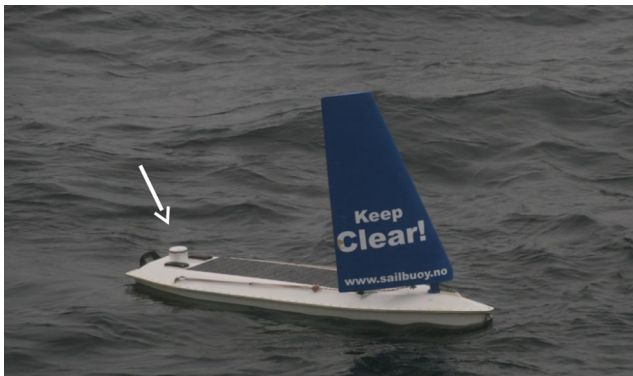
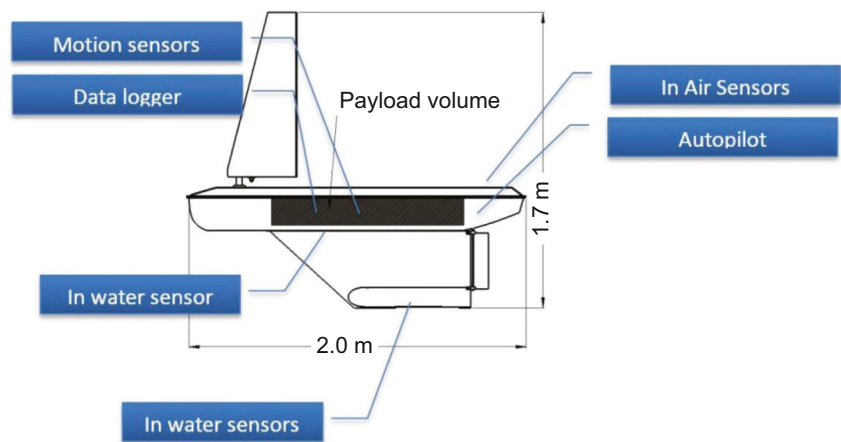
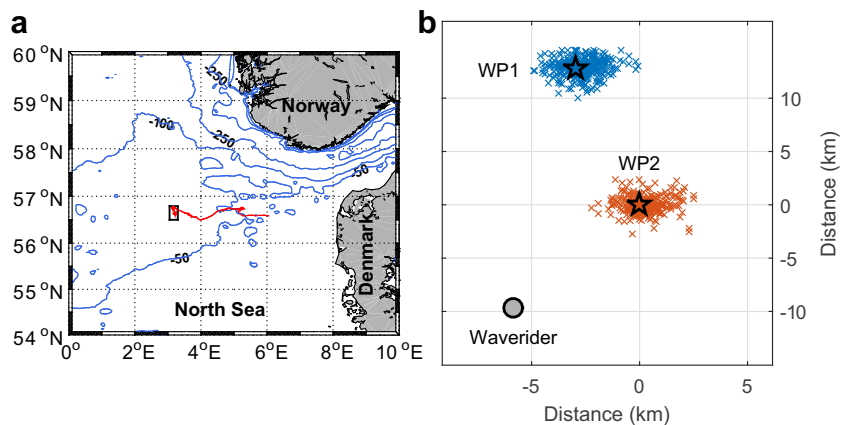


**Fig. 2** Picture taken on 2 November 2015 showing the SB Wave. The wave sensor's GPS antenna is marked by an *arrow*

2011). There is high shipping density and substantial offshore oil activity in the area. Multiple offshore wind farms are under development and detailed information about the wave climate has practical and economical value, since construction dimensioning off shore is dependent on wave climate information.

**Fig. 3** Maps showing the mission of SB Wave (a) together with the waypoints WP1 and WP2 and station keeping around them (b). The *bullet* marks the position of the Waverider buoy, approximately 10 km south of WP2



Accurate ocean wave measurements are important for verification of ocean wave forecasts and wave climate mapping (Steward 2008). The observation network at sea is coarse, and there is a consistent lack of wave measurements to verify model predictions (Reistad et al. 2005). Long-term in situ wave monitoring programmes tend to be interrupted as a result of environmental stresses such as bio-fouling and severe weather (Herbers et al. 2012; Manov et al. 2004).

Wave-forecasting models in use by meteorological agencies are based on integrations of the directional wave spectrum discretized in direction and frequency (or wavenumber), (See e.g. Komen et al. 1994 or Steward 2008). The forecasts follow individual components of the wave spectrum in space and time, allowing each component to grow or decay depending on advection, energy input by local winds, energy sinks by dissipation, such as wave breaking and bottom friction, and repartition of energy by non-linear interactions. Detailed and accurate wave measurements to validate these models are consequently of interest.

Ocean waves are measured remotely by observing the sea state, by satellite altimeters (Queffeuou 2004) or by

**Table 1** Measurement positions and duration

	Position (latitude; longitude)	Measurement period (2015, UTC)
WP1	56° 45.0' N; 3° 9.0' E	7 November 0000–14 November 1000
WP2	56° 38.1' N; 3° 11.9' E	14 November 1200–20 November 0930
Waverider	56° 32.9' N; 3° 6.2' E	Entire mission

Synthetic Aperture Radars (SAR) (Li et al. 2008). In situ measurements are normally carried out by accelerometers or Global Positioning System (GPS) sensors mounted on floating buoys (e.g. Jeans et al. 2003) or, in the case of shallow water, Acoustic Doppler Current Profilers (ADCPs) or other wave gauges mounted on the sea floor (Herbers and Lentz 2010). Alternative methods, such as mounting of ADCPs on autonomous underwater vehicles (Haven and Terray 2015), the Surpact Waverider (Reverdin et al. 2013), and ship-mounted acoustic sensors (Christensen et al. 2013) have also been demonstrated.

Here we describe a novel methodology, namely a GPS-based 2 Hz motion sensor mounted on a small

autonomous surface vehicle. This configuration can have advantages such as low costs (no ship time needed), independence of water depth, flexibility, and mobility. Other advantages using GPS based sensors are size, robustness, and no need of calibration (Herbers et al. 2012). The measurement platform is tested over a period of about 2 weeks during rough weather conditions in the Central North Sea and measurements are compared to observations carried out by a permanently installed traditional Waverider. The main aim of this study is to test the Sailbuoy for its operational capability for measuring wave parameters in rough ocean conditions.

**Fig. 4** Environmental parameters observed at Ekofisk during the experiment.  $H_s$  is significant wave height, while  $T_p$  is the peak period, the wave period with the highest energy, both measured by the Waverider. Start and end times (vertical lines) and durations (horizontal lines) of WP1 and WP2 stations occupied by the Sailbuoy are indicated

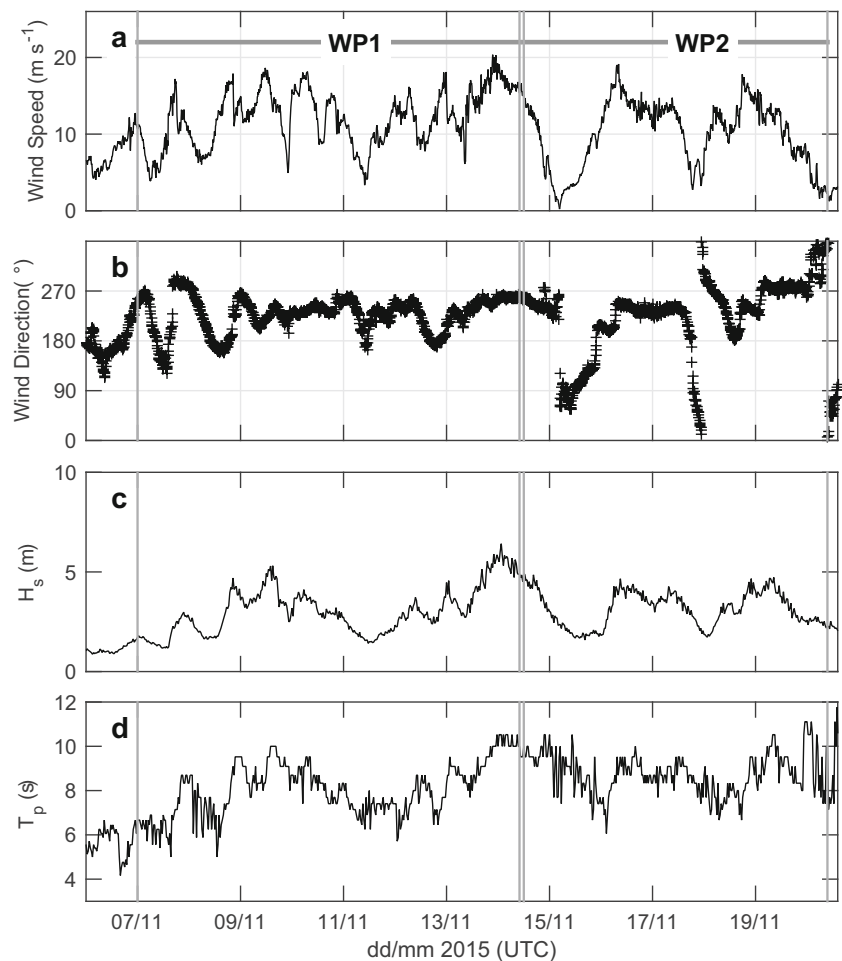
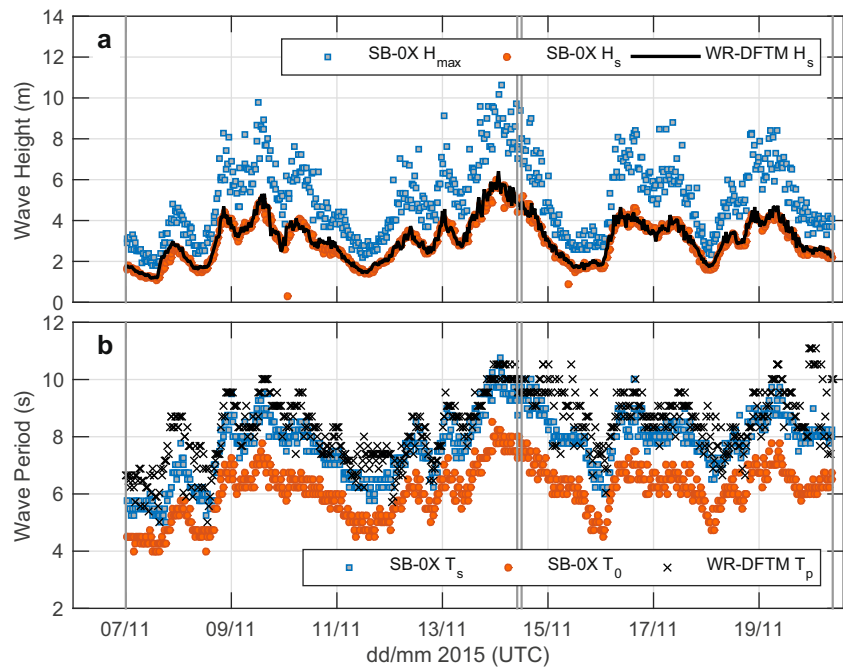


**Fig. 5** Time series of wave parameters relayed by Iridium; internally processed using the zero-crossing method compared to Ekofisk Waverider observations processed by the direct Fourier transform method (DFTM). Vertical lines mark the start and end times of WP1 and WP2



## 2 Method

The Sailbuoy (Figs. 1 and 2) is an unmanned surface vehicle (USV) manufactured by Offshore Sensing AS ([www.sailbuoy.no](http://www.sailbuoy.no)). It navigates autonomously and uses wind power for propulsion. Data communication and control are in real-time, including data relay, established using the Iridium satellite system. The Sailbuoy is specifically designed for use in Norwegian waters (e.g. North Sea and Barents Sea), for robustness with the ability to survive and operate in very rough environmental conditions (wind, waves and temperature). It can be deployed and retrieved by untrained personnel from light vessels. The physical dimensions are 2 m length, 60 kg displacement and a payload of 15 kg (60 l). It can be fitted with various sensors to be used for a wide variety of ocean applications including near-surface temperature, salinity and oxygen concentration monitoring, chemical sensors, and wave measurements.

The Sailbuoy has proven its endurance and navigation capability through various missions including a transect from Bergen, Norway to Iceland, Bergen to Scotland, a mission north of Svalbard close to the marginal ice zone, and surveys in the northern Gulf of Mexico and off Gran Canaria. For a report on the navigation capability and efficacy we refer to Fer and Peddie (2012), for a report on near-surface temperature, salinity and oxygen concentration measurements see Fer and Peddie (2013) for an application in the northern Gulf of Mexico see Ghani et al. (2014).

For the experiment described here, the Offshore Sensing Sailbuoy Wave (SB Wave hereafter) was equipped with the Datawell MOSE-G1000 wave sensor ([www.datawell.nl](http://www.datawell.nl)). This is a three-dimensional motion sensor based on single GPS and measures the translational motion of the GPS antenna in three frequency or period regimes each with its own precision: high-frequency motion (1–100-s periods, 1 cm precision), low frequency motion (10–1000 s periods, several cm precision), and GPS position

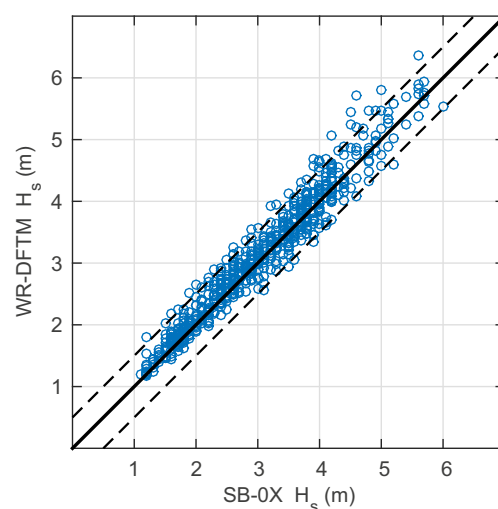
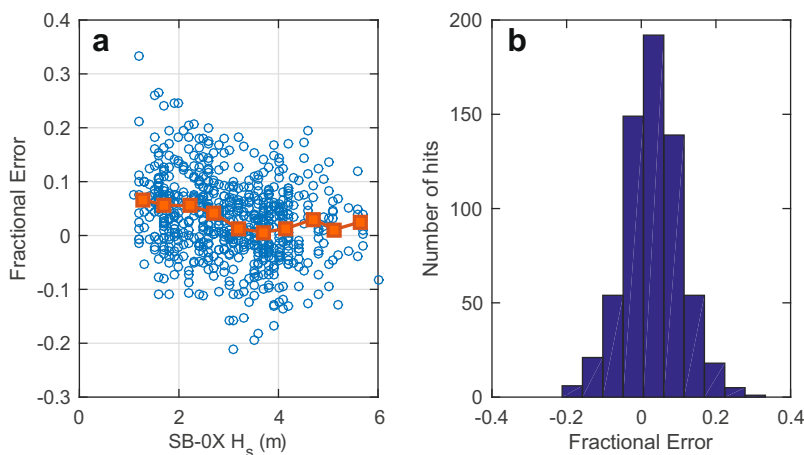


**Fig. 6** Scatter plot of significant wave height ( $H_s$ ) relayed by Iridium; internally processed data using the zero-crossing method (SB-0X) compared to Ekofisk Waverider observations processed by DFTM (WR-DFTM)

**Fig. 7** Fractional error of internally processed  $H_s$  using the zero-crossing method relative to the Ekofisk Waverider measurements. **a** Distribution with respect to  $H_s$ ; *circles* all data points; *squares*, averaged in 0.5 m bins of  $H_s$ , **b** histogram of fractional error



(infinitely long periods, 10 m precision). An indoor version of the sensor was installed in the payload section of the SB Wave, and the external GPS antenna was integrated at the rear part of the buoy (Fig. 2). The antenna is free from obstructions and is elevated above the deck to mitigate potential signal loss due to wave wash over. For details on the MOSE-G1000 we refer to the manufacturer’s reference manual.

The reference measurements at the Ekofisk platform are from a Datawell non-directional Waverider.

### 3 Deployment

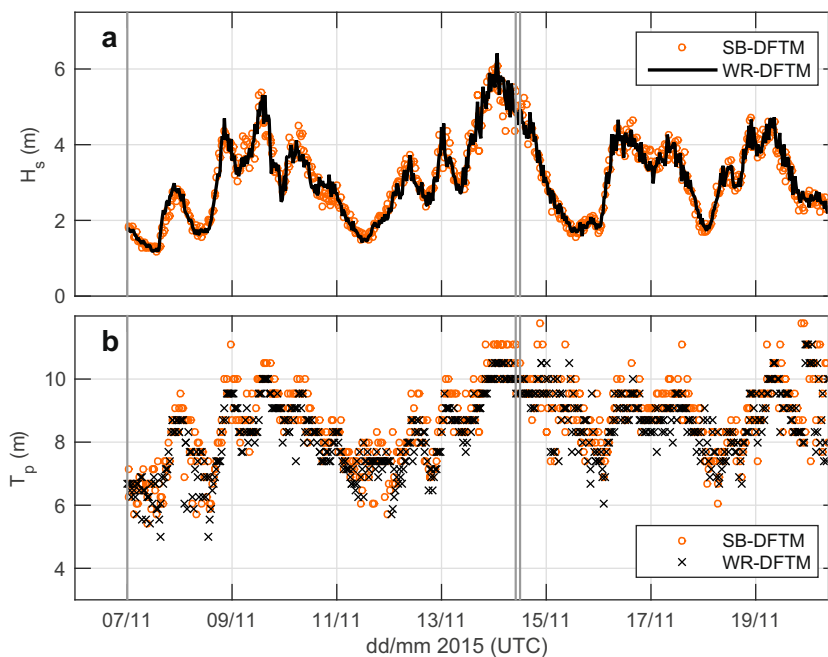
The SB Wave was deployed during a cruise of the research vessel *Håkon Mosby* (cruise number HM2015 623), on 30

October 2015, 18:00 UTC, at 56° 32' N along the track of the vessel towards the FINO1 platform in the North Sea. Ekofisk is in block 2/4 of the Norwegian sector of the North Sea about 320 km southwest of Stavanger (Fig. 3a).

The Sailbuoy was directed to the way point WP1 to keep station and conduct wave measurements. On 14 November, the Sailbuoy was directed to WP2, closer to a nearby bottom-anchored conventional wave buoy (Waverider). The position and measurement periods are summarised in Table 1. The mission is shown together with way point and Waverider positions in Fig. 3. The Sailbuoy was recovered on 20 November 2015.

The Sailbuoy was successful in station keeping and maintained a position within  $\pm 2$  km of the way points (Fig. 3b).

**Fig. 8** Times series of **a** significant wave height and **b** peak wave period from the post-processed raw data using DFTM (SB-DFTM, *orange*) compared to Ekofisk Waverider observations processed by DFTM (WR-DFTM, *black*). *Vertical lines* mark the start and end times of WP1 and WP2





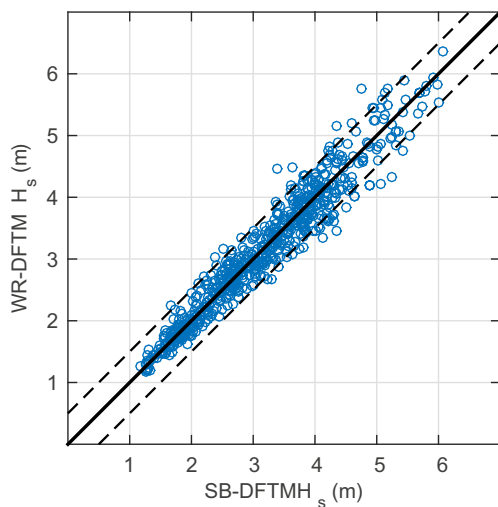


**Fig. 9** Scatter plot of significant wave height from post-processed raw SB Wave data using DFTM compared to Ekofisk Waverider observations processed by DFTM

The MOSE-G1000 sensor was set to sample at 2 Hz. The internal logging included the high-frequency (HF) string containing horizontal and vertical displacements and a data quality flag. Furthermore, every 10 s the position, together with horizontal dilution of precision (HDOP) and vertical dilution of precision (VDOP), were logged. The sensor was initialized by power (82 mA), and a new data file was written every 30 min, logging data for 25 min (3000 data points). The sensor was left on continuously, thanks to the short duration of the experiment. While the entire raw data field was logged internally, the data were also transferred to the Sailbuoy for data reduction and relay of wave parameters via satellite. The first 125 data points (of 3000; approximately 1 min) were excluded to avoid a possible contamination by filter effects or file book-keeping.

There are, therefore, two data sets as follows: (1) full resolution, raw sensor data for post processing using

various methods to infer wave parameters, and (2) twice-hourly real-time relayed data including time, position and key wave parameters inferred onboard from a zero-crossing analysis of typically 2875 data points. For further details on the data processing and reduction, see Fer and Peddie (2016).

The internal processing of 2875 data points every 30 min follows the following steps:

- (i) detect individual waves using zero-crossing of the vertical displacement record (retain every second zero-crossing to define a complete wave, this is loosely referred to as the number of zero-crossings),
- (ii) calculate wave height and wave period for each individual wave,
- (iii) sort the wave heights (book-keeping the corresponding periods),
- (iv) calculate the significant wave height ( $H_s$ , average of the largest 1/3rd sorted wave heights) and the maximum wave height ( $H_{max}$ ), and
- (v) calculate mean zero-crossing period ( $T_0$ , mean period of all the waves in the record), and the significant period ( $T_s$ , average period of the waves used to define  $H_s$ ).

In addition to these parameters, the total number of data points, the number of bad data points (quality flag bad from the sensor) and a sensor on/off flag are sent. The data return is very good, despite the large waves (Fig. 4). In each segment, there are approximately between 200 and 300 zero-crossings (individual waves). When  $H_s$  is less than approximately 3 m, there are no erroneous data points. Such bad data are expected, for example, when seawater covers the GPS antenna which may happen at high seas. Even when the maximum wave height is about 10 m, the number of bad data returns is on the order 100, which is less than 3 % of the segment length (Fer and Peddie 2016). This small amount of data loss has

**Fig. 10** Fractional error of post-processed from SB Wave raw data using DFTM relative to the Ekofisk Waverider measurements. **a** Distribution with respect to  $H_s$ : circles all data points; squares, averaged in 0.5 m bins of  $H_s$ , **b** histogram of fractional error

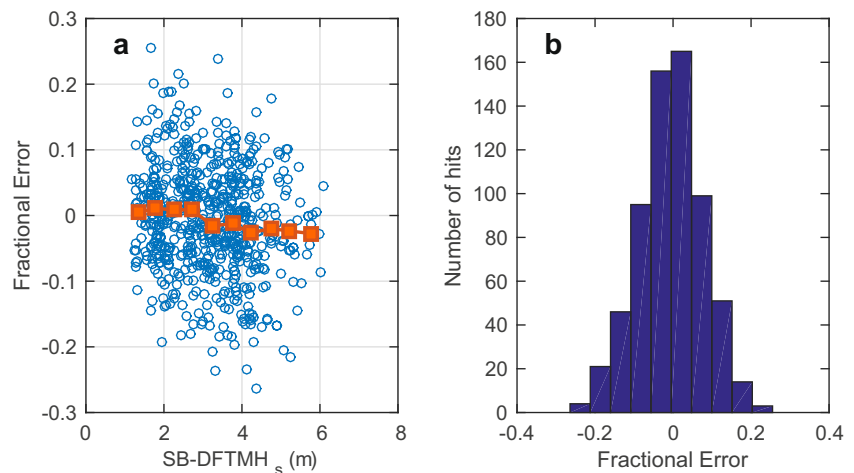


**Table 2** Statistics of SB Wave to Waverider comparison for significant wave height,  $H_s$

WP	$n$	$r$	Bias (m)	MAE (m)	RMSE (m)	MPE (%)	MPAE (%)
All	654	0.97	-0.010	0.20	0.27	-0.6	6.5
WP1	361	0.97	-0.020	0.22	0.29	-1.2	7.1
WP2	289	0.96	-0.007	0.18	0.24	-0.3	5.7

Bias is the mean signed difference between the time series. WP2 was approximately 10 km from the Waverider, while WP1 was approximately 20 km from the Waverider

$n$  number of data points,  $r$  linear correlation coefficient, *MAE* mean absolute error, *MPE* mean percent error, *MPAE* mean percent absolute error, *RMSE* root-mean-square error

negligible (unquantified) influence on the resulting wave parameter estimates.

### 4 Results and discussion

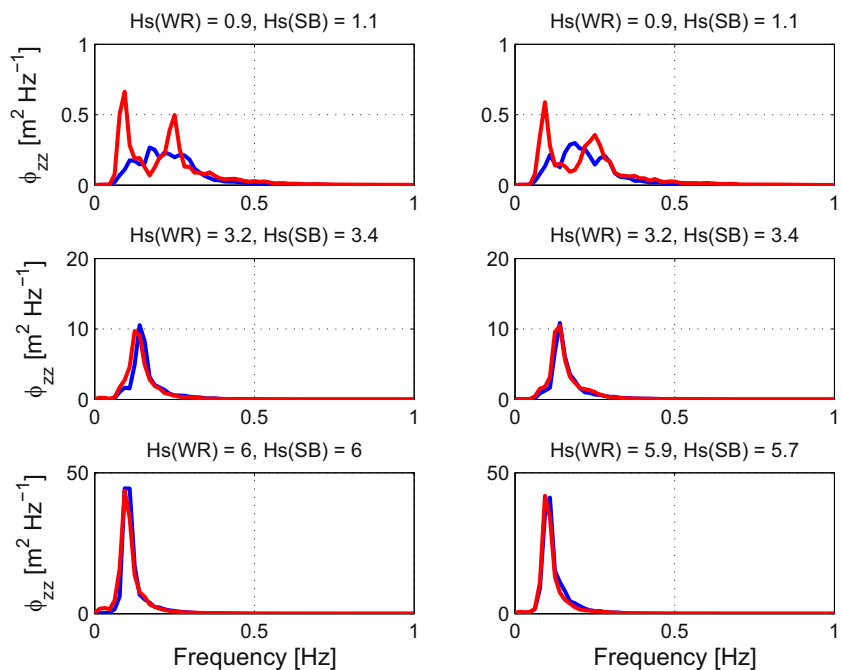
The period of deployment was dominated by a series of passing lows to the west of Ekofisk and the predominant wind direction was southwest, as common for the season. This means that SB Wave was mostly downwind of Ekofisk. Mean wind speed over the 14 days of deployment was 9.8 m/s ( $U_{10m}$ —10 min average), with a maximum wind speed of 21.4 m/s on 13 November 2130 UTC (Fig. 4). Given the vigorous wind conditions, we assume that the

relative contribution of swell was minor during the field campaign.

We use the Waverider observations as reference, and compare the SB Wave measurements against Waverider measurements. First, a comparison is made using real-time SB Wave data obtained using the zero-crossing method described in Section 3. Next, a comparison is made using the post-processed SB Wave data (spectral processing using the direct Fourier transform method, DFTM, described below). Internally processed zero-crossing results are compared to the Waverider observations to showcase the accuracy of the real-time data relayed by the Sailbuoy. Waverider measurements were interpolated to the Sailbuoy time stamps and provided 654 measurement points (Figs. 5, 6 and 7). The fractional error between SB Wave and the Waverider does not show a trend with increasing  $H_s$  (Fig. 7a), indicating that SB Wave is robust in different wave regimes. However, it has not been tested for very high waves ( $H_s > 10$  m), which is quite rare even in the North Sea (Aarnes et al. 2012). One would expect increased error for increasing  $H_s$ , for example, because of increased number of bad data points or failure to detect individual waves by the zero-crossing method, but this is not observed.

Raw data downloaded from the instrument are further analysed for more accurate estimates of the wave parameters, using spectral analysis. For spectral analysis of both SB Wave and Waverider data we used the DIWASP Matlab toolbox ([www.metocean.co.nz](http://www.metocean.co.nz)) and the direct Fourier transform method (DFTM) originally developed by

**Fig. 11** Comparison of spectra (power spectral density,  $\Phi_{zz}$ ) from Sailbuoy Wave at WP1 (SB) and the Waverider (WR). Significant wave heights ( $H_s$ ) for six cases are given in the plots. The six cases are 20-min segments starting at the following times (from upper left): 02 November, 01:25:43, 02 November, 01:55:43, 12 November, 06:55:43, 12 November, 07:25:43, 13 November, 22:55:51 and 13 November, 23:25:51. The Sailbuoy is tacking (sailing against the wind) for all cases, except the middle left panel



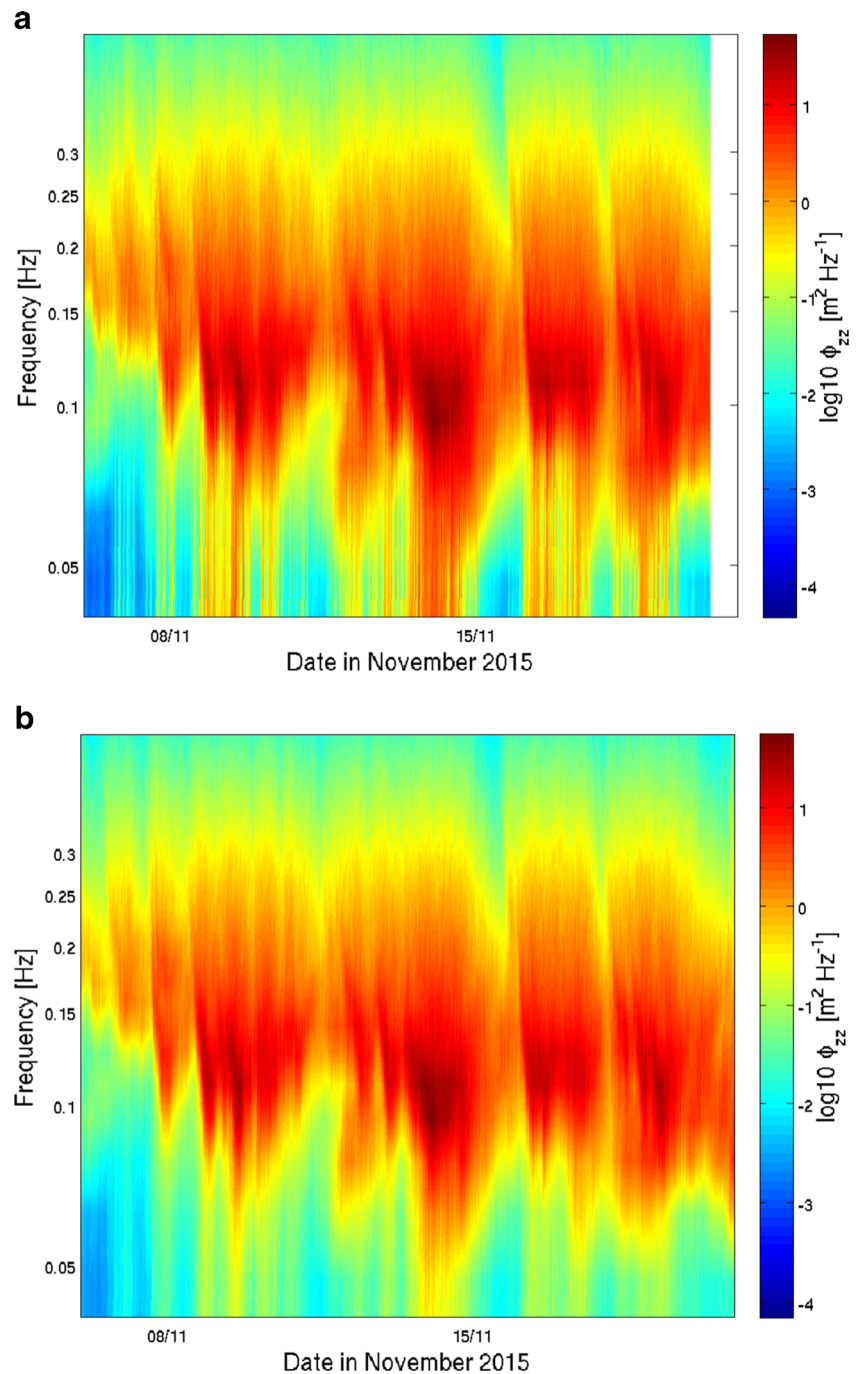
Barber (1961). DFTM is used with a frequency resolution of 0.01 Hz in the range 0.05 to 1 Hz, and a direction resolution of  $2^\circ$ . Note, however, that the Waverider is non-directional, and the directional spectra are calculated for SB Wave only. From the analysis, the significant wave height,  $H_s$ , peak period,  $T_p$ , and for SB Wave, direction of spectral peak,  $D_{Tp}$  and the dominant direction,  $D_p$  are extracted.

The agreement between the wave parameters measured by the two platforms is very good, lending confidence on the Sailbuoy measurements (Figs. 8, 9 and

10, and Table 2). Linear correlation coefficient between the two time series of  $H_s$  is 0.97 ( $r^2=0.94$ ). When analysed separately measurements from WP1 and WP2, respectively 20 km and 10 km from the Waverider, give results statistically identical  $r=0.97$  and  $r=0.96$ , respectively. Given the horizontal distance between SB Wave and the Waverider at Ekofisk, the spatial coherence is satisfactory.

Power spectral density for six selected samples of the two measurement systems were calculated using the method of Welch (1967), which has efficient noise reduction.

**Fig. 12** Spectrogram (power spectral density obtained from **a** SB Wave and **b** Waverider. The colour scale is logarithmic





Spectral comparison for medium (~3.3 m) and high (~6 m)  $H_s$  cases is shown in Fig. 11 and also shows good comparison. However, for the low  $H_s$  case (~1 m), the SB Wave spectrum seems to be influenced by the motion of the Sailbuoy itself, with peaks at 0.1 and 0.25 Hz. This may be due to non-linearities as suggested by Barrick and Steele (1989) and Hara and Karachintsev (2003). Internal motion of the Sailbuoy is masked out at higher wave heights. However, we do not have enough information to separate the pitch, roll and heave of the vessel from the acceleration caused by the waves.

Spectrograms for the entire campaign from SB Wave and the Waverider are shown in Fig. 12, using the Welch (1967) method for both datasets. The energetic period around 14 November is visible in both spectrograms and the temporal patterns are similar, where a low frequency contribution ( $T_p$  of 10–12 s) is present most of the time. In energetic segments, the SB Wave spectra show bands of elevated energy (red) extending to low frequencies (<0.05 Hz) which is not present in the Waverider data.

The SB Wave spectra are also shown in Fig. 13, where each spectrum is colour coded for the average wind speed during the measurement, following Thompson et al. (2013). It is clearly seen that the peaks in the spectra shift to lower frequencies with higher wind speeds. Also, the higher frequency parts of the spectra between about 0.1 and 0.6 Hz follow the  $f^{-4}$  slope in the equilibrium range as first suggested by Toba (1973). This observation is somewhat different from that of Hara and Karachintsev (2003) who suggest an  $f^{-5}$  dependence for the wind sea part of the spectrum. The noise above 0.6 Hz could be

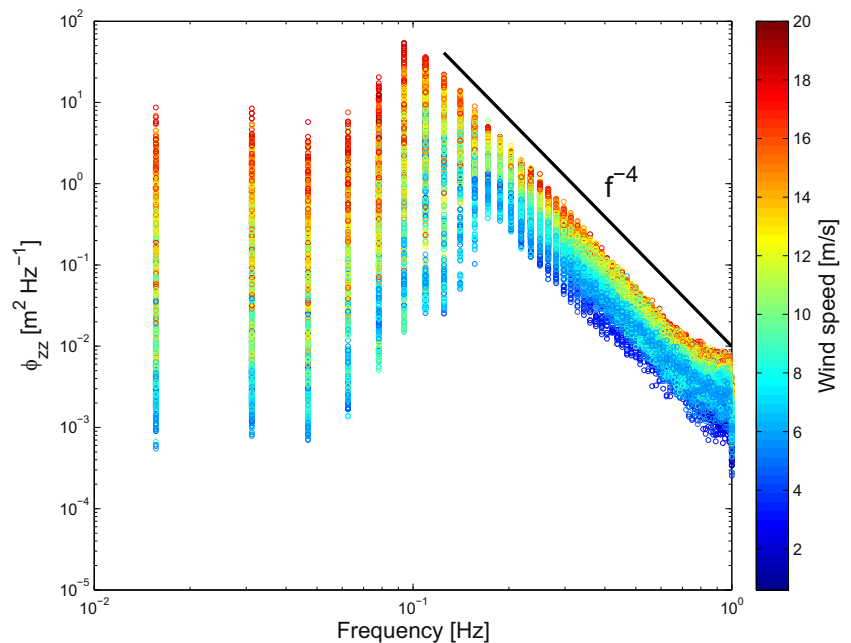
due to motion of the Sailbuoy’s hull, but the energy levels are here very low. This noise is not visible in the linear plot in Fig. 11.

Since the Ekofisk Waverider is non-directional, wave direction comparison is not possible. However, in Fig. 14, we show rose plots of the peak period direction,  $D_{TP}$ , coloured for  $H_s$ , together with a rose plot of wind directions observed at Ekofisk, coloured for wind speeds. Wave directions are here defined as the propagation direction. It is clearly seen that the prevailing southwesterly wind results in waves propagating towards the northeastern sector.

Finally, examples of directional spectra from SB Wave (calculated by DIWASP and the DFTM method) are shown in Fig. 15. The six examples are the same segments as in Fig. 11. Two examples for low (~1 m), moderate (~3.2 m) and high  $H_s$  (~6 m) are shown to demonstrate consistency in the measurements of energy distribution in frequency and direction. It appears that SB Wave is able to observe rather well-defined wave directions, even in vigorous seas. In the upper two panels, a weak swell propagating towards the southeast can be observed together with wind sea propagating towards the northeast.

The Sailbuoy kept station during most of this campaign, and it was tacking (sailing into the wind) 71 % of the time. Since it moved typically 100 m between each 30 min sampling, the speed while keeping station was approximately 0.05 m/s. Given that the typical wave speed is 100 times higher, it seems reasonable that the Doppler shift can be ignored as long as the Sailbuoy keeps station. In Fig. 11, all but the middle left panel are sampled during tacking. In the middle left panel, SB

**Fig. 13** Sailbuoy wave energy spectra colour coded by mean wind speed for each spectrum



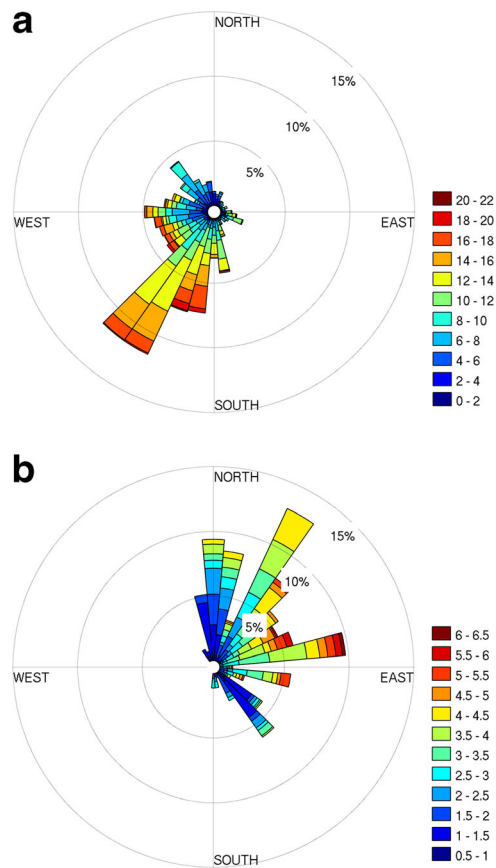


**Fig. 14** **a** Rose plots of Ekofisk wind directions colour coded for wind speed (m/s). **b** Sailbuoy wave directions colour coded for  $H_s$  (m)

Wave sailed downwind with a speed of approximately 1 m/s, so a slight Doppler shift could be expected and may be discernible in the comparison with the Waverider spectrum, but the difference may also be due to horizontal separation. The SB measures a somewhat higher  $T_p$  than the WR (mean difference of 0.29 s)(Fig. 8). For the periods when the SB sails upwind (71 % of the time), the difference is slightly lower (0.26 s), while for downwind sailing the difference is 0.35 s. The small difference between upwind and downwind sailing suggests that there is no significant Doppler effect.

## 5 Summary and conclusion

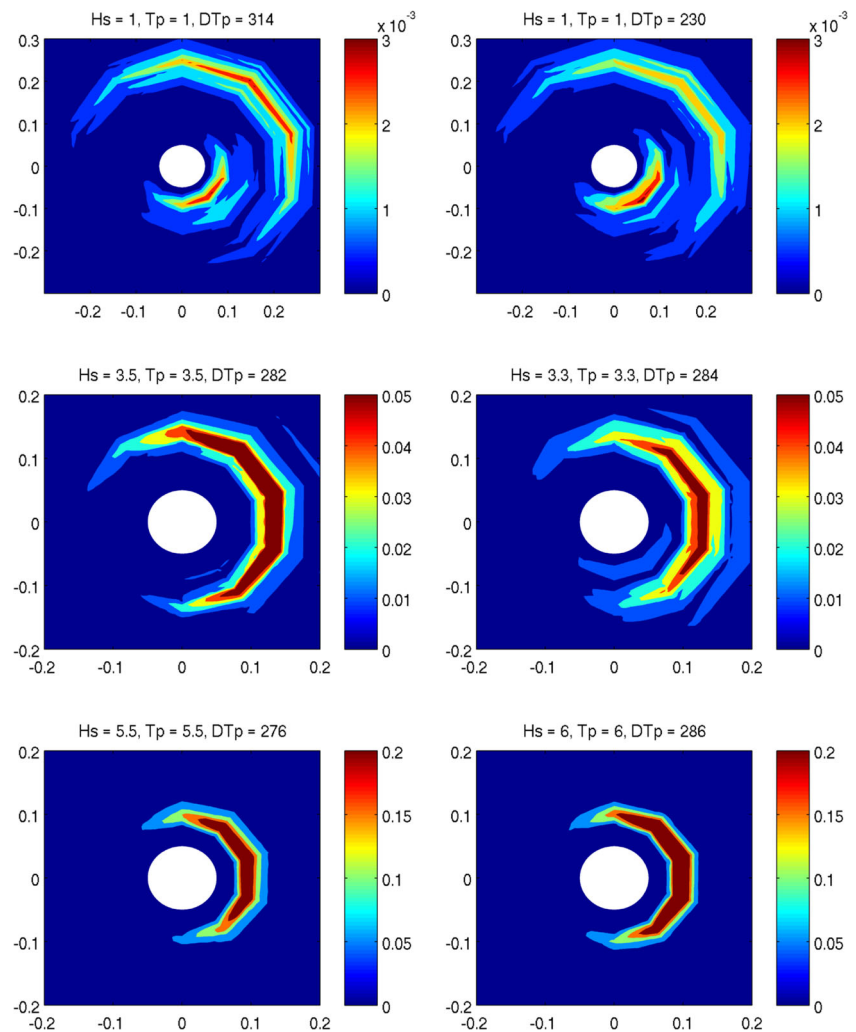
Recent developments in global positioning system (GPS) technology have enabled in situ ocean wave measurements at a relatively low cost using surface-following buoys (Herbers et al. 2012). In the experiment presented here, a Datawell MOSE G1000 sensor was placed in an autonomous vessel, the Offshore Sensing Sailbuoy. A data set was collected between 7 and 20 November 2015, near the Ekofisk oil field in the North Sea. For sensor inter

comparison and data validation, the measurement position was co-located (10 to 20 km) with a bottom-anchored Waverider buoy. The measurement period covers from quiescent periods with  $H_s$  on the order 1 m to energetic periods with  $H_s$  reaching 6 m with maximum wave heights in excess of 10 m. The peak period of the wave spectrum was approximately 5 s for the  $H_s$  on the order 1 m, and 10–12 s for  $H_s$  exceeding 5 m.

The Sailbuoy delivered two data sets as follows: (i) twice-hourly real-time relayed wave parameters processed on board using a zero-crossing analysis; and (ii) full resolution, raw sensor data for post processing using spectral methods to infer wave parameters. First, the real-time data set is compared with the Waverider measurements to showcase the operational merit of the Sailbuoy. The agreement is very good with a fractional error less than 10 %, and without a significant trend when binned in  $H_s$ .

Next, the wave measurements from the Sailbuoy are compared with the Waverider measurements using spectral analysis of 30 min time series of 2 Hz sampling rate. The agreement between the two data sets is good with a linear correlation coefficient of 0.97, a bias of 1 cm, a root-mean-square error

**Fig. 15** Post-Processed directional wave spectra measured by the Sailbuoy for cases of low, moderate and high waves (the same cases as Fig. 11).  $H_s$ ,  $T_p$  and  $D_{Tp}$  are indicated in the plots. The Sailbuoy is tacking (sailing against the wind) for all cases, except the middle left



of 27 cm, and a mean percent absolute error of 7 %. The observations presented here suggest that the Sailbuoy is a suitable platform for wave measurements delivering reliable real time data as well as accurate post-processed data. This is particularly true for spectral measurements for medium (~3 m) and high (~6 m) wave heights and for integrated values ( $H_s$ , and  $T_p$ ).

The advantages of using GPS based wave sensors have already been discussed by Herbers et al. (2012). A GPS based sensor placed in the Sailbuoy could be a particularly attractive and cost-efficient alternative for short term measurement programmes (weeks to months) carried out as part of coastal and offshore construction project planning.

The emerging possibility to use robust autonomous platforms for wave measurements at relatively low costs provides an opportunity for more dense wave observations in the future, of benefit for forecasters and commercial users. The main aim of this study is to test the Sailbuoy for its operational capability for measuring wave parameters in rough ocean conditions. Future studies should involve focus on hull effects on measurements of

low and high-frequency waves, comparison with other directional sensors as well as the use of multiple platforms for mapping of horizontal coherence.

**Acknowledgments** This study is partly funded by the Norwegian Centre of Offshore Wind Energy (NORCOWE). The Waverider raw data and the wind data have kindly been provided by the operator of Ekofisk, ConocoPhillips. The deployment of the Sailbuoy was conducted from a University of Bergen research cruise. We thank ConocoPhillips and Skandi Marøy for retrieving the Sailbuoy at Ekofisk, and two reviewers for their comments on the manuscript.

**Open Access** This article is distributed under the terms of the Creative Commons Attribution 4.0 International License (<http://creativecommons.org/licenses/by/4.0/>), which permits unrestricted use, distribution, and reproduction in any medium, provided you give appropriate credit to the original author(s) and the source, provide a link to the Creative Commons license, and indicate if changes were made.

## References

- Aarnes OJ, Breivik Ø, Reistad M (2012) Wave extremes in the northeast Atlantic. *J Clim* 25(5):1529–1543
- Barber, NF (1961) The directional resolving power of an array of wave detectors, *Ocean Wave Spectra*. Prentice Hall. Inc. pp.137-150
- Barrick DE, Steele KE (1989) Comments on “Theory and application of calibration techniques for an NDBC directional wave measurements buoy” by KE Steele, et al.: nonlinear effects. *Ocean Eng IEEE J* 14(3):268–272
- Christensen KH, Röhrs J, Ward B, Fer I, Broström G, Sætra Ø, Breivik Ø (2013) Surface wave measurements using a ship-mounted ultrasonic altimeter. *Methods Oceanogr* 6:1–15
- Fer I, Peddie D. (2012) Navigation performance of the Sailbuoy. Bergen - Scotland mission, 12 pp. [www.sailbuoy.no](http://www.sailbuoy.no)
- Fer I, Peddie D (2013) Near surface oceanographic measurements using the Sailbuoy. *OCEANS 2013 MTS/IEEE, IEEE*, 15
- Fer I, Peddie D (2016) Report on wave measurements using the Sailbuoy wave. [www.sailbuoy.no/files/Report\\_Ekofisk\\_Nov2015.pdf](http://www.sailbuoy.no/files/Report_Ekofisk_Nov2015.pdf)
- Ghani MH, Hole LR, Fer I, Kourafalou VH, Wienders N, Kang H, Drushka K. and Peddie D (2014) The Sailbuoy remotely-controlled unmanned vessel: measurements of near surface temperature, salinity and oxygen concentration in the Northern Gulf of Mexico. *Methods in Oceanography*, 10, 104-121, doi: <http://dx.doi.org/10.1016/j.mio.2014.08.00>
- Grabemann I, Weisse R (2008) Climate change impact on extreme wave conditions in the North Sea: an ensemble study. *Ocean Dyn* 58(3-4): 199–212
- Hara T, Karachintsev AV (2003) Observation of nonlinear effects in ocean surface wave frequency spectra. *J Phys Oceanography* 33(2):422–430
- Haven S, & Terray EA. (2015) Surface wave measurements from an autonomous underwater vehicle. In *Current, Waves and Turbulence Measurement (CWTM)*, 2015 IEEE/OES Eleventh (pp. 1-7). IEEE
- Herbers THC, Jessen PF, Janssen TT, Colbert DB, MacMahan JH (2012) Observing ocean surface waves with GPS-tracked buoys. *J Atmos Ocean Technol* 29(7):944–959
- Herbers THC, Lentz SJ (2010) Observing directional properties of ocean swell with an acoustic Doppler current profiler (ADCP). *J Atmos Ocean Technol* 27(1):210–225
- Jeans G, Bellamy I, de Vries JJ, & van Weert P (2003) Sea trial of the new Datawell GPS directional Waverider. In *Current Measurement Technology, 2003. Proceedings of the IEEE/OES Seventh Working Conference on* (pp. 145-147). IEEE
- Komen G, Cavaleri L, Donelan M, Hasselmann K, Hasselmann S, & Janssen PAEM (1994) *Dynamics and Modelling of Ocean Waves*
- Li XM, Lehner S, He MX (2008) Ocean wave measurements based on satellite synthetic aperture radar (SAR) and numerical wave model (WAM) data—extreme sea state and cross sea analysis. *Int J Remote Sens* 29(21):6403–6416
- Manov DV, Chang GC, Dickey TD (2004) Methods for reducing bio-fouling of moored optical sensors. *J Atmos Ocean Technol* 21(6): 958–968
- Reistad M, Magnusson AK, Haver S, Gudmestad OT, Kvamme D (2005) How severe wave conditions are possible on the Norwegian Continental Shelf? *Mar Struct* 18(5):428–450
- Reverdin G, Morisset S, Bourras D, Martin N, Lourenço A, Boutin J, Salvador J (2013) Surpact: a SMOS surface Waverider for air-sea interaction. *Oceanography* 26(1):48–57. doi:[10.5670/oceanog.2013.04](https://doi.org/10.5670/oceanog.2013.04)
- Steward HR (2008) *Introduction to physical oceanography*. Department of Oceanography. A & M University, Texas. [http://oceanworld.tamu.edu/resources/ocng\\_textbook/PDF\\_files/book.pdf](http://oceanworld.tamu.edu/resources/ocng_textbook/PDF_files/book.pdf)
- Thomson J, D’Asaro EA, Cronin MF, Rogers WE, Harcourt RR, Shcherbina A (2013) Waves and the equilibrium range at Ocean Weather Station P. *J Geophys Res Oceans* 118:5951–5962. doi:[10.1002/2013JC008837](https://doi.org/10.1002/2013JC008837)
- Toba Y (1973) Local balance in the air-sea boundary processes. III. On the spectrum of wind waves. *J Oceanogr Soc Jpn* 29:209–220
- Queffelec P (2004) Long-term validation of wave height measurements from altimeters. *Mar Geodesy* 27(3-4):495–510
- Welch PD (1967) The use of fast Fourier transform for the estimation of power spectra: a method based on time averaging over short, modified periodograms. *IEEE Trans Audio Electroacoust* 15(2):70–73
- Young IR, Zieger S, Babanin AV (2011) Global trends in wind speed and wave height. *Science* 332(6028):451–455